Materials Chemistry and Physics 264 (2021) 124433

Contents lists available at ScienceDirect

Materials Chemistry and Physics

journal homepage: www.elsevier.com/locate/matchemphys

Thiosemicarbazide-modified/ion-imprinted phenolic resin for selective uptake of cadmium ions

Nadia H. Elsayed [a,b,*], M. Monier [c,d,**], Raedah A.S. Alatawi [e]

[a] Department of Chemistry, University College-Alwajh, University of Tabuk, Tabuk, Saudi Arabia
[b] Department of Polymers and Pigments, National Research Centre, Dokki, Cairo 12311, Egypt
[c] Chemistry Department, Faculty of Science, Mansoura University, Mansoura, Egypt
[d] Chemistry Department, College of Science, Taibah University, Yanbu Branch, Yanbu El-Bahr, Saudi Arabia
[e] Department of Chemistry, Faculty of Science, University of Tabuk, Tabuk 71421, Saudi Arabia

HIGHLIGHTS

- Active thiosemicarbazide modified salicylic acid (H_2TCS) ligand was synthesized and coordinate with Cd^{2+} ions.
- The prepared $[CdTCS(H_2O)_3]$ complex was implemented in condensation polymerization with resorcinol and formaldehyde.
- The resulted ion-imprinted resin was characterized by various instrumental methods.
- The resin was applied to selectively remove Cd^{2+} ions from aqueous solutions.

GRAPHICAL ABSTRACT

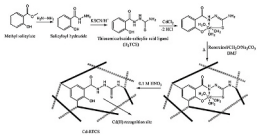

ARTICLE INFO

Keywords:
Thiosemicarbazide
Salicyloyl hydrazide
Cadmium (II) ions
Ion-imprinting

ABSTRACT

Cd(II)-imprinted Cd(II) resin obtained from a thiosemicarbazide derivative of salicylic acid was prepared and evaluated for selective uptake of Cd(II) ions. In the beginning, the thiosemicarbazide derivative of salicylic acid (H_2TCS) was developed as a functional ligand that was then coordinated with Cd(II) ions to obtain the Cd-complex $[CdTCS(H_2O)_3]$. After the full investigation of the ligand and its complex, they copolymerized with resorcinol in presence of formalin, and the obtained resinous material was eluted with 0.1 M HNO_3 solution to extract the polymer incorporated Cd(II) ions and finally produce the Cd(II) ions selective Cd-RTCS sorbent. The maximum cadmium ions capacity by the Cd-RTCS reached 164 ± 1 mg/g, which could be a relatively high and promising value. Also, the adsorption isotherms were interpreted better with the Langmuir model. In addition, the Cd(II) sorption using Cd-RTCS was tested in a competitive medium of Pb(II), Ni(II), Zn(II), and, Cu(II) ions and the results indicated a considerable selectivity toward the Cd(II) ions over the coexisted metals.

1. Introduction

Cadmium (Cd) is a highly poisonous heavy metal that represents a high risk to human health if it exists, even in trace quantities in food sources or drinking water, which may be contaminated as a result of cadmium leakage into the environment from various industrial wastes

* Corresponding author. Department of Chemistry, University College-Alwajh, University of Tabuk, Tabuk, Saudi Arabia.
** Corresponding author. Chemistry Department, Faculty of Science, Mansoura University, Mansoura, Egypt.
E-mail addresses: nhussein@ut.edu.sa (N.H. Elsayed), monierchem@yahoo.com (M. Monier).

https://doi.org/10.1016/j.matchemphys.2021.124433
Received 1 December 2020; Received in revised form 17 February 2021; Accepted 18 February 2021
Available online 23 February 2021

[1]. The presence of cadmium as a trace pollutant in the food chain has proven to cause many types of cancer and therefore, international health organizations including WHO and FAO have determined the permissible quantities of cadmium at 25 μg per month for every 1 kg of the body weight [2]. Consequently, it is necessary to develop and update techniques for estimating and extracting cadmium from potentially contaminated food and drink sources [3,4]. Several techniques such as adsorption [5], ion exchangers [6], and liquid extraction [7] were recently employed in the separation and preconcentration, which significantly overcomes the low sensitivity and interference problems.

Among these technologies, adsorption is the most attractive in economic as well as in terms of efficiency [8]. However, the lack of selectivity for most commonly used sorbents including active carbon significantly reduces the extraction efficiency towards specific target species [9]. Thus, the ion-imprinted polymers, which possess excellent selective performance, have recently become an object of study and development of many researchers [10–13].

The idea of ion-imprinting is mainly dependent on the template-supported synthesis of the selective recognition cavities within the construction of a polymeric network. When extracting the ionic template, the recognition cavities left are largely identical to the expelled ions due to the static orientation of the chelating groups during the polymerization reaction as well as the radius and ionic shape, which can acquire the obtained polymeric network remarkable selective characteristics towards the targeted metal ions [14–21]. While fabricating the ion-imprinted polymers, the targeted metal ion is coordinated to a chelating monomeric ligand forming a complex that further involved in a copolymerization process with a suitable cross-linking agent [22]. After that, the process of extracting ions from the polymer network must be done very carefully, as the ions must be removed only while maintaining the shape and stability of the binding sites [23]. Many techniques including suspension, condensation, sol-gel, and graft copolymerization have been used in the imprinting of various metal ions [24–27]. For example, Pb(II) imprinted material functionalized with vinyl pyridine and methacrylic acid was developed for extracting Pb(II) ions from water [28]. Acrylic acid modified chitosan was utilized in developing Ni(II) ion-imprinted carbon nanotubes [29]. Polyvinylimidazole-silica functionalized ion-imprinted hybrid material was prepared for removal of Pb(II) ions [30]. 3-mercaptopropyltrimethoxylane/4-vinylpyridine combination was employed in the development of Cd(II) imprinted material [31]. In conclusion, ease of processing, inexpensive raw materials, as well as high durability and stability, which enhances the chances of reuse many times, are all important advantages that favor the use of this technology [32–34].

This paper presents the development of Cd(II) imprinted phenolic resins (Cd-RTCS) that able to target and selectively capture Cd(II) ions in aqueous solutions. The synthetic steps start with the synthesis of the thiosemicarbazide derivative of salicylic acid (H_2TCS) that can effectively form a stable complex with the Cd(II) ions. The imprinted Cd-RTCS resin was then prepared through condensation polymerization of a mixture of the synthesized Cd-complex, resorcinol, and formalin followed by extracting the resin incorporated Cd(II) ions. The synthesized ligand and its corresponding Cd(II) ion complex were fully characterized to assure the chemical changes. In addition, the stability and morphology of the obtained resin were also examined before evaluating its Cd(II) ions binding affinity.

2. Material and methods

2.1. Chemicals

Methyl salicylate (99%), resorcinol (99%), potassium thiocyanate, hydrazine hydrate solution (80%), formalin solution (37%), and all utilized metal ions have been supplied from Sigma-Aldrich (USA). Solvents and other reagents have been supplied from various companies.

2.2. Synthesis of thiosemicarbazide-salicylic acid ligand (H_2TCS)

The synthesis of the H_2TCS ligand was inspired by previous work [35]. 5 mL methyl salicylate was added to a mixture of 5 mL methanol and 2 mL hydrazine hydrate. The reaction flask was shaken for 1 h at 50 °C then left to stand at 30 °C. The formed salicyloyl hydrazide was precipitated as white crystals that were filtered and washed with cold methanol. In the next step, 4 g of the prepared hydrazide derivative was mixed with 20 mL ethyl alcohol and stirred until complete dissolution. The solution was then joined to a reflux system at 60 °C. In another vial, 3 g potassium thiocyanate was dissolved in 20 mL ethanol acidified with 1 mL HCl solution (0.5 M) then gradually added to the first salicyloyl hydrazide solution and the reaction continued under reflux and stirring at 60 °C. The formation of the H_2TCS was detected by TLC and after 6 h; the obtained precipitate was filtered and recrystallized using isopropyl alcohol with yields around 90% and melting point 188–190 °C.

2.3. Synthesis of the Cd^{2+} complex [$CdTCS(H_2O)_3$]

The complex was prepared by mixing the 4 g of H_2TCS and 3.5 g $CdCl_2$ in 20 mL ethyl alcohol. The reaction was accomplished by heating under reflux and stirring at 75 °C, within 2 h the [$CdTCS(H_2O)_3$] complex start to precipitate. The reflux continued for an additional 2 h then [$CdTCS(H_2O)_3$] was separated and rinsed with ethyl alcohol then dried for the subsequent investigation and processing.

2.4. Polymerization

The condensation polymerization was carried out in the dimethylformamide (DMF) solvent (30 mL) where a mixture of 4 g [$CdTCS(H_2O)_3$] complex, 1.2 g resorcinol, and sodium carbonate solution (5 mL, 25% (w/v)) was added and shaken until one phase solution is observed. The formaldehyde solution (10 mL) was then blended before refluxing the reaction contents for 5 h at 100 °C. The gelled resinous materials were then separated, washed with DMF and ethanol, and dried in the open air for 12 h before grinding and sifting at an average size of 200 μm. The ground pellets were then shaken with dilute HNO_3 solution (0.1 M) for 1 h at 30 °C to extract the resin incorporated Cd(II) ions and the treatment was performed multiple times to ensure the entire elimination of the cadmium (II) ions. The sorbent has been then neutralized by immersing in 0.1 M aq. NaOH before rinsing with distilled water and storing for the subsequent characterization and examination steps. All the previous procedures were repeated using H_2TCS instead of the [$CdTCS(H_2O)_3$] to prepare a control blank NI-RTCS resin sorbent. Scheme 1 presents the synthesis and polymerization steps.

To assure accordance and reproducibility of the results of the studies, the synthesis of all the above materials was first performed with small amounts in preliminary experiments and were all investigated before preparing the large batches.

2.5. Characterization

The quantities of the main elements C, H, N, and S were obtained as percentages for both H_2TCS and [$CdTCS(H_2O)_3$] on a Perkin–Elmer 240 C Elemental Analytical Instrument (USA). The amount of cadmium in the [$CdTCS(H_2O)_3$] complex was determined according to the standard method [36] as described in the following. 0.1 g of the [$CdTCS(H_2O)_3$] was mixed with 5 mL concentrated nitric acid and the mixture was boiled for 10 min. Distilled water was added to dilute the solution to 25 mL and the free Cd(II) ions were quantified by ICP technique on an Agilent 7500 instrument (USA) and by EDTA titration. Also, H_2TCS and [$CdTCS(H_2O)_3$] were examined using ICP-MS Portfolio instrument to record the mass spectra. The [$CdTCS(H_2O)_3$] complex was dissolved in DMSO to record the electronic spectrum in a range 200–900 nm using Unicam UV2 UV–visible spectrometer. NMR spectra of H_2TCS and [$CdTCS(H_2O)_3$] in DMSO-d_6 solvent were obtained by Oxford NMR

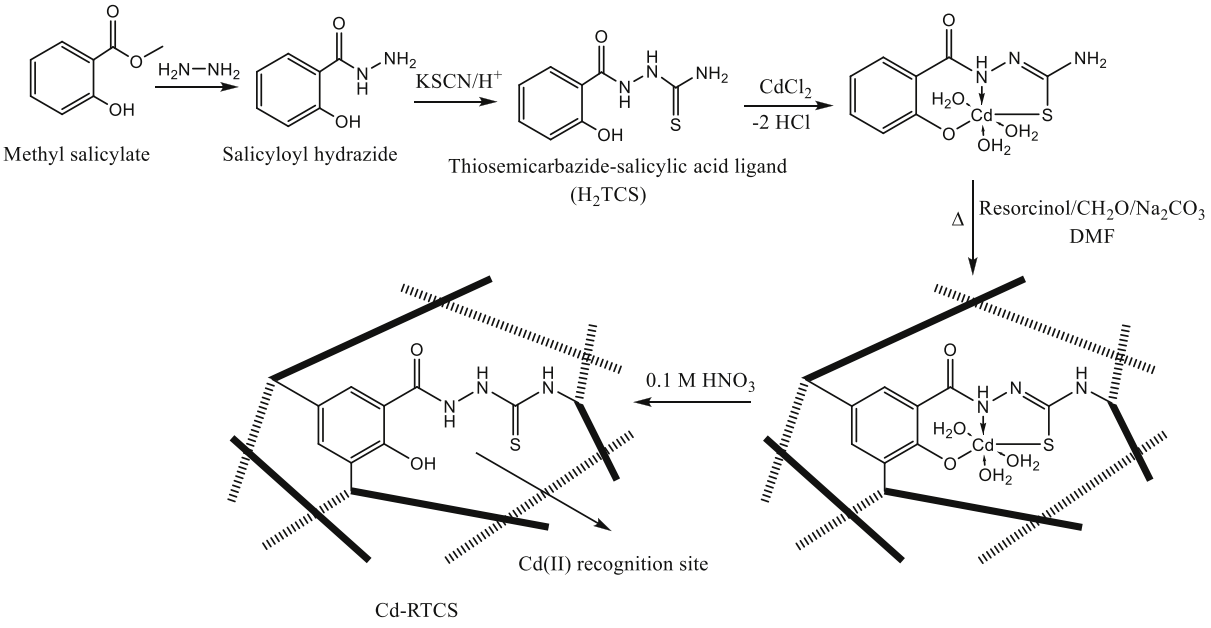

Scheme 1. Schematic presentation for the synthetic steps of Cd-RTCS.

instrument (Model Unity Inova 500 MHz, USA). Fourier transforms infrared spectra (FTIR 500-4000 cm^{-1}) of the H_2TCS, [$CdTCS(H_2O)_3$], Cd-RTCS, and NI-RTCS were all recorded to identify the functional group changes on a Perkin–Elmer instrument fitted with an ATR accessory. The surface morphology of Cd-RTCS and NI-RTCS was characterized after coating with gold on scanning electron microscope (SEM) (FEI Quanta-200, Netherlands) at operating voltage 20 kV. The Brunauer-Emmett-Teller (BET) surface area of the Cd-RTCS and NI-RTCS were measured on ASAP 2010 Micromeritics instrument. Energy-dispersive X-ray (EDX) spectra of Cd-RTCS before and after Cd (II) ions elution was obtained using HITACHI S-4800, Japan EDX instrument.

2.6. Cd(II) ions uptake experiments

The equilibrium uptake capacity of the sorbents Cd-RTCS and NI-RTCS were examined using batches prepared by incubating 50 mg of the sorbent with 50 mL, 10–400 mg/L Cd(II) ions solution. Diluted NaOH and HCl solutions were utilized in adjusting the pH at the desired values and after shaking the batch bottles for the desired period of time at 30 °C, the residual Cd(II) ion contents in the aqueous phase was estimated by ICP-MS method to quantify the extracted Cd(II) ions according to the following equations.

$$q_e = \frac{(C_i - C_e)V}{W} \quad (1)$$

where C_i and C_e are the initial and equilibrium Cd(II) ions concentrations (mg/L) in the adsorption batch solution, V is the volume of the adsorption batch (L), and W is the used adsorbent weight (g).

2.7. Selectivity studies

The specific recognition capability of the Cd-RTCS for selective binding with Cd(II) was tested in presence of some common competitive ions including Pb(II), Ni(II), Zn(II), and, Cu(II) which possess similar valence and close ionic size with our targeted Cd(II) ions [37]. The experiment was executed by immersing 0.05 g of the Cd-RTCS in a 50 mL aqueous solution containing the above-mentioned competitive ions beside the Cd(II) with concentrations of 30 mg/L for each one. The pH adjusted to 6.0 and the batch was equilibrated at 30 °C and 200 rpm for 3 h. After the batch was settled samples of the aqueous solution were withdrawn to analyze the metal ion contents using ICP. The control batch experiment was repeated under the same conditions but by using NI-RTCS. The selectivity parameters are then calculated utilizing the following equations [38]:

$$\text{Distribution coefficient, } D = \frac{C_i - C_f}{C_f} x \frac{V}{W} \quad (2)$$

$$\text{Selectivity coefficient, } \beta_{Cd^{2+}/M^{n+}} = \frac{D_{Cd^{1+}}}{D_{M^{n+}}} \quad (3)$$

$$\text{Relative selectivity coefficient, } \beta_r = \frac{\beta_{imprinted}}{\beta_{non-imprint}} \quad (4)$$

where C_i and C_f are the initial and final metal ion concentrations in the adsorption system. D^{2+}_{Cd} is the distribution coefficient of Cd^{2+} ions; D^{n+}_{M} is the distribution coefficient of the interfering ions.

2.8. Selective removal of Cd(II) from the Ni-Cd battery effluents

The solid effluents of the Ni-Cd battery (5 g) were treated with 10% (w/v) sulfuric acid (100 mL) for 6 h under magnetic stirring at 70 °C. The mixture was then left to cool at 30 °C before adding 10 mL H_2O_2 solution 10%(w/v). The aqueous phase was then separated by filtration and completed to 500 mL by distilled water then the pH was adjusted at 6, and finally the Cd(II) and Ni(II) ions concentrations were determined [34]. In two different batches, 50 mL of the above waste solution and 50 mg of either Cd-RTCS or NI-RTCS sorbents were mixed with and the batches were equilibrated at 30 °C and 200 rpm for 2 h, and then the remained contents of the two metal ions were measured.

2.9. Regeneration

The Cd(II) ions loaded Cd-RTCS sorbent resin was eluted by shaking with 0.1 M nitric acid solution at 30 °C for 2 h. Then the resin was removed and washed with distilled water until neutralization and then dried and reused in a new Cd(II) removal experiment. This process was performed 5 consecutive times with the same adsorbent sample and every time the adsorption capacity was determined.

3. Results and discussion

3.1. Characterization

The molecular weight of the [CdTCS$(H_2O)_3$] complex was obtained from the mass spectrum, which demonstrated M+1 peak at $m/z = 374.9$. In addition, the quantities of the main elements C, H, N, and S that were obtained as percentages from the elemental analysis beside the Cd(II) ions amount in the complex that was determined after digestion with nitric acid are presented in Table 1 and as can be seen, all the element contents are in agreement with the suggested chemical structures presented in Scheme 1.

FTIR spectra were used to clarify the manner of coordination through which Cd(II) is chelated by the H_2TCS and the main peaks that undergoing diagnostic changes after the complex formation are presented in Table 2. It is a known fact at first that the thioamide (NH-C=S) moiety of thiosemicarbazide enables the occurrence of thion-thiol tautomeric forms in solution (Structure 1) [39]. The observed peaks around 1255 and 880 cm^{-1} that belong to the C=S and the peak at 3400 cm^{-1} that characterize the phenolic O-H along with the absence of any peaks around 2300 and 1150 cm^{-1} that are supposed to characterize S-H and C-S bonds, respectively in the spectrum of the H_2TCS revealed the dominance of the thion tautomer in solid-state. Furthermore, the spectrum of the [CdTCS$(H_2O)_3$] displayed the C-S peaks around 1150 and 660 cm^{-1} beside the occurrence of a C=N peak around 1650 cm^{-1}, while the characteristic C=S and O-H peaks at 1255, 880, and 3400 cm^{-1}, respectively, have been almost vanished. These findings confirmed that the phenolic –OH and the thiosemicarbazide moieties have mainly participated in the Cd(II) chelation via thion-thiol transformation and deprotonation of both –OH and –SH groups.

The complex [CdTCS$(H_2O)_3$] electronic spectrum (Fig. 1) demonstrated only a band at 340 nm that related to charge transfer of $^2Eg \rightarrow {}^2T_2$ g transition, suggesting an octahedral coordination geometry [40].

Fig. 2 presents the ^{1}H NMR spectra of H_2TCS and [CdTCS$(H_2O)_3$]. The free ligand spectrum presented a signal pattern that characterizes the o-disubstituted benzene system containing multiple signals at 6.9 ppm, triplet signal at 7.4 ppm, and doublet signal at 7.7 ppm beside the signals at 7.3, 8.3, 9.0, and 9.5 ppm, which can be related to –NH_2, –NH–NH–, and -OH protons, respectively. This spectrum also reveals the dominance of the thion tautomer as suggested by the FTIR spectrum. The [CdTCS$(H_2O)_3$] spectrum displayed significant peak shifts. Moreover, one of the hydrazide protons and the phenolic –OH proton are vanished, which also confirms the previously suggested Cd(II) chelation mechanism via thion-thiol transformation and deprotonation of both –OH and –SH groups.

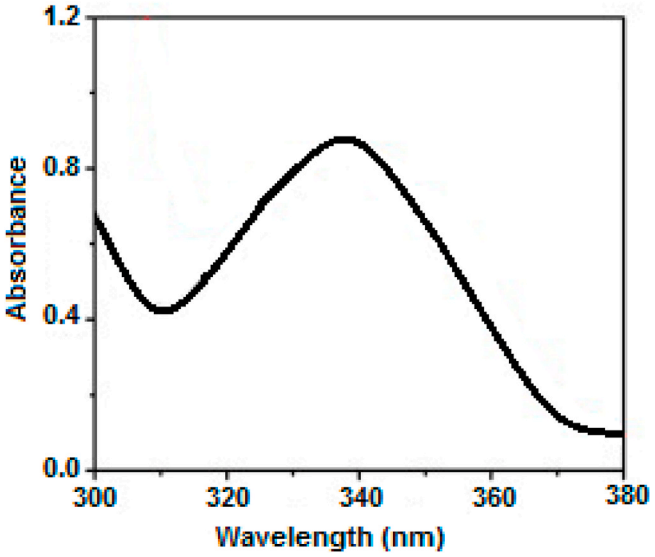

Fig. 1. Electronic spectrum of [CdTCS$(H_2O)_3$] complex.

Furthermore, Fig. 3 shows the ^{13}C NMR spectra of H_2TCS and [CdTCS$(H_2O)_3$]. The observed signal shifts of the C=O and C=N can give additional evidence for the Cd(II) chelation according to the suggested mechanism.

The suggested structures of H_2TCS thion-thiol tautomers and [CdTCS$(H_2O)_3$] are theoretically optimized on Hyperchem 8.0 software via MM+ and semi-empirical PM3 forcefield method and the optimized conformations are shown in Structure 1. As expected, thion tautomer is much more stable than thiol form by 81.21 kJ/mol, which is in agreement with both FTIR and NMR instrumental results. In addition, the [CdTCS$(H_2O)_3$] complex displayed octahedral coordination, and the polymerization sites in both free –NH_2 and aromatic ring are in positions that allow the molecular approach without steric hindrance.

The surfaces of the prepared Cd-RTCS and NI-RTCS resin materials were also photographed by SEM (Fig. 4), which demonstrated a relatively regular and smooth appearance in the case of NI-RTCS in comparison to the roughness of the observed pore surface in the case of Cd-RTCS. These observations are found to match with the measured surface area of both resin types that were 65.334 and 206.453 m^2/g for NI-RTCS and Cd-RTCS, respectively. The chemical alternations that accompanying the elution of the Cd(II) ions from the internal texture of the Cd-RTCS resin can explain this observed rough morphology and consequently this higher surface area. Indeed, the extraction and separation of ionic species by adsorption require the provision of maximum accessibility between the target ions and the adsorbed active sites, which can only be achieved by increasing the absorption surface area. Thus, the observed pore morphology with this relatively high surface area of Cd-RTCS is an advantage during the Cd (II) removal process.

The stability of the coordination groups within the Cd-RTCS is evaluated by matching the FTIR charts of the NI-RTCS, Cd-RTCS before and after Cd(II) elution (Fig. 5). The spectrum of the Cd(II)/Cd-RTCS demonstrated a similar spectrum with that related to [CdTCS$(H_2O)_3$] suggesting the polymer incorporation of Cd(II) ions through the same chelation mode. Moreover, the spectra of both NI-RTCS and Cd(II) free Cd-RTCS demonstrated an almost identical spectral pattern. This confirms that the chelating groups are stable and unaffected during the Cd

Table 1
Elemental analysis of H_2TCS and [CdTCS$(H_2O)_3$].

Found (calc.) (%)					
Compound	C	H	N	S	Cd
H_2TCS	24.9 (45.5)	4.2 (4.3)	20.1 (19.9)	15.4 (15.2)	–
[CdTCS $(H_2O)_3$]	25.8 (25.6)	3.3 (3.5)	12.0 (11.2)	9.0 (8.5)	29.7 (30.0)

Table 2
Characteristic IR bands (cm^{-1}) of the ligand H_2TCS and complex [CdTCS $(H_2O)_3$].

Compound	ν(O-H)	ν(C=N)	ν/δ(C=S)	ν/δ(C-S)
H_2TCS	3400	–	1255, 880	–
[CdTCS$(H_2O)_3$]	-	1650	-	1150, 660

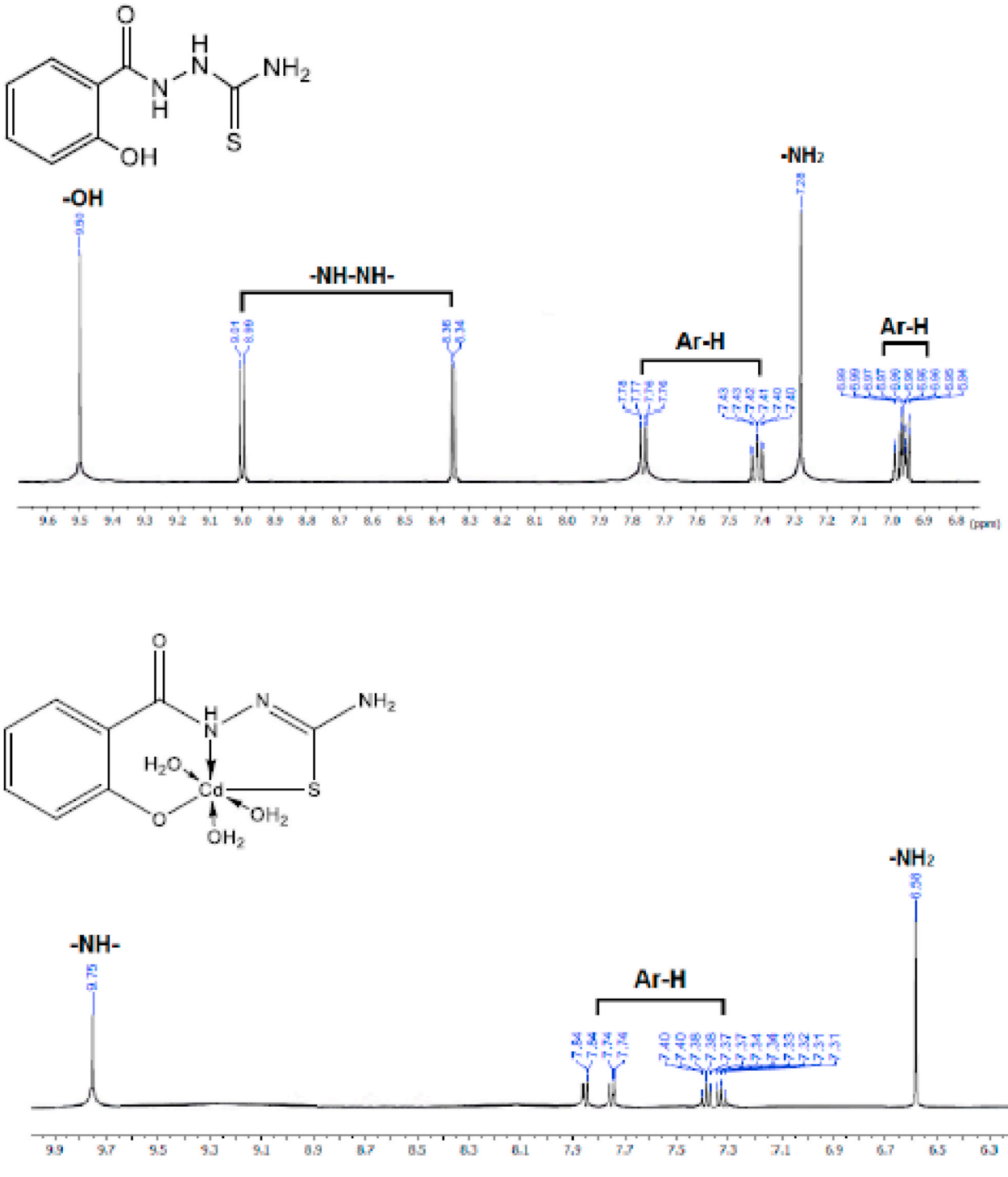

Fig. 2. ^{1}HNMR spectra of (a) H_2TCS, (b) $[CdTCS(H_2O)_3]$.

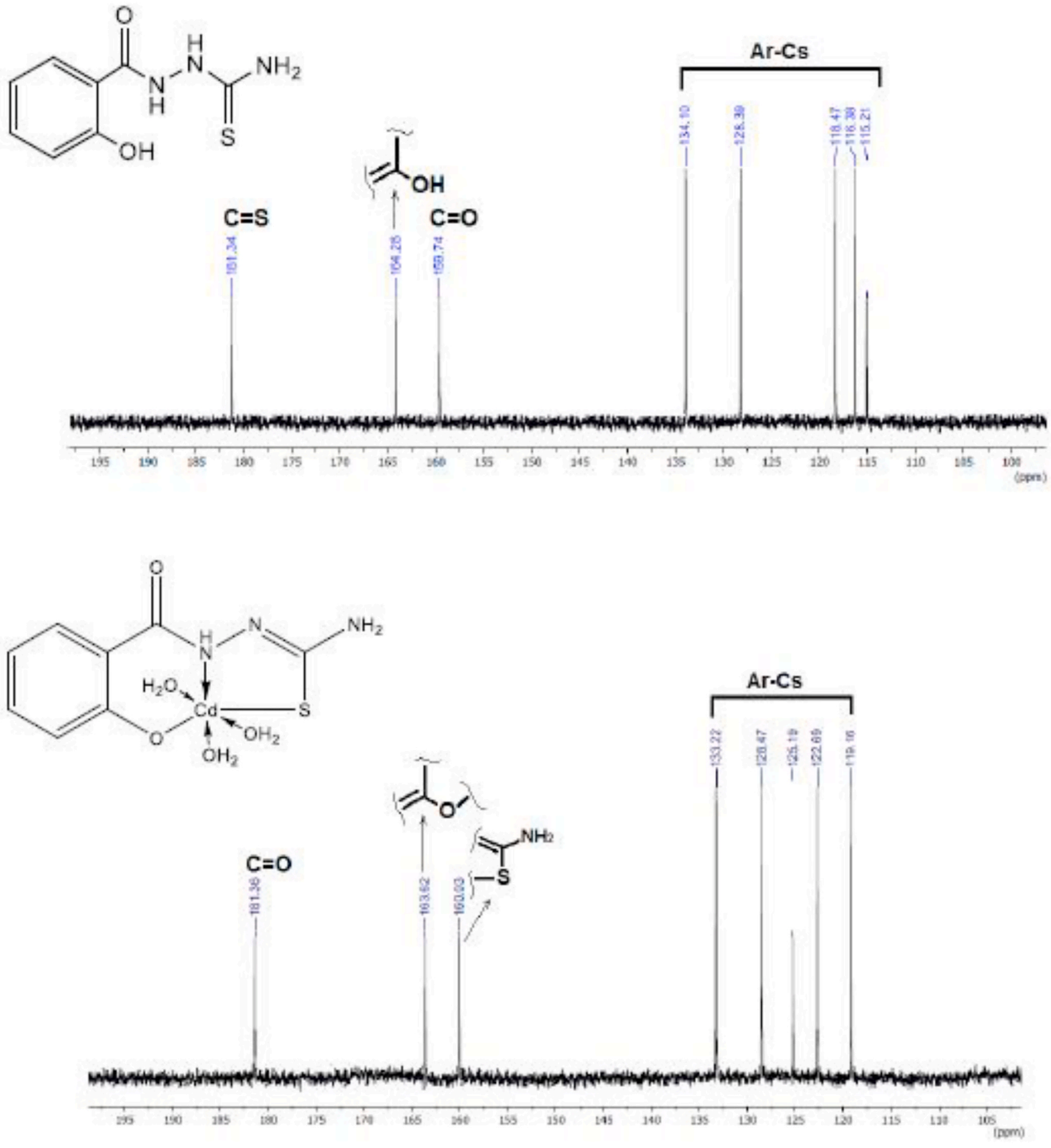

Fig. 3. ^{13}C NMR spectra of (a) H_2TCS, (b) $[CdTCS(H_2O)_3]$.

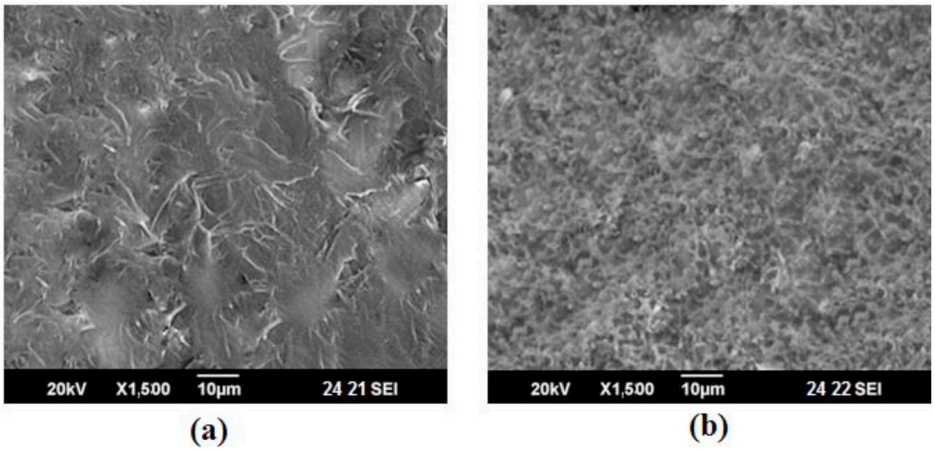

Fig. 4. SEM photos of (a) NI-RTCS (b) Cd-RTCS.

(II) elution process.

The efficiency of the Cd(II) desorption using 0.1 M nitric acid solution was also evaluated by scanning the Cd-RTCS resin before and after Cd(II) elution using EDX spectroscopy (Fig. 6), which reveals the complete elimination of the Cd(II) upon the performed HNO_3 processing by the disappearance of the characteristic cadmium peaks that were present prior to elution.

3.2. Cd(II) ions removal studies

3.2.1. Effect of pH

The removal capacity of both Cd-RTCS and NI-TRCS sorbents are significantly influenced by the initial pH value of the working Cd(II) ion batch solution. Fig. 7 showed that the adsorbed amounts of the Cd(II) ions by both sorbents are greatly increased by raising the pH value up to 6, above this value, the Cd(II) ions start to precipitate as hydroxide, thus the optimum pH value was chosen at 6 in all of the next experiments. The weak adsorption abilities of both adsorbent types under acidic environments are expected and could be attributed to the high abundance of the H^+ ions, which can compete and occupy the chelating sites and resist coordination of the targeted Cd(II) ions. Moreover, under all investigated conditions, Cd-RTCS displayed a higher capacity compared to the NI-RTCS sorbent, which can be attributed to the relatively more irregular and porous morphology of the Cd-RTCS that incorporated with the imprinted Cd(II) ions chelating sites.

3.2.2. Adsorption isotherms

Usually, the adsorbate-adsorbent interaction mechanism is better understood by performing the adsorption isotherms. The Cd(II) ions adsorption isotherms on Cd-RTCS and NI-RTCS are presented in Fig. 8, which indicated experimental maximum capacities 164 ± 1, and 73 ± 1 mg/g for both Cd-RTCS and NI-RTCS, respectively. The observed higher Cd-RTCS capacity may be related to the previously discussed irregular morphological appearance and the higher surface area beside the presence of the Cd(II) recognition sites. Moreover, Table 3 collected the Cd (II) ions maximum capacities related to some recently reported ion-imprinted materials and compare it to the obtained value in our current Cd-RTCS adsorbent and it is clear that the capacity of the current material is promising and competitive.

The adsorption behavior could be elucidated by considering Freundlich and Langmuir models in the mathematical treatment of the experimental results.

Freundlich [41].

$$\ln q_e = \ln K_F + \frac{1}{n} \ln C_e \quad (5)$$

Langmuir [42].

$$\frac{C_e}{q_e} = \frac{1}{K_{L q_m}} + \frac{C_e}{q_m} \quad (6)$$

where K_F is the Freundlich constant, $1/n$ is the adsorption index, C_e (mg/L) is the Cd(II) ions concentration after equilibration, q_e (mg/g) is the equilibrium adsorption capacity, and q_m (mg/g) is the maximum adsorption capacity.

The modeling performance of both equations with both Cd-RTCS and NI-RTCS adsorbents are presented in Table 4 and accordingly, with the obtained higher R^2 values in the case of the Langmuir equation, it is suggested that the Cd(II) ions adsorption by both adsorbents is better described by the Langmuir than Freundlich models. Thus, the Cd(II) ions are adsorbed by strongly equivalent coordination sites on the Cd-RTCS and NI-RTCS surfaces.

Also, as shown in the isotherms, under low initial Cd(II) ions concentrations, the adsorption displayed a linear tendency, and the q_e increases by increasing the Cd(II) concentration. According to the IUPAC classification, these isotherms are L-type [43] where the adsorbent reaches saturation progressively after the monolayer formation.

3.2.3. Cd(II) ions uptake kinetics

The rate of the Cd(II) ions adsorption using both Cd-RTCS and NI-RTCS beside the essential kinetic constants was determined by constructing the kinetic curves via plotting the Cd(II) ions adsorbed amounts versus the time (Fig. 9). As can be noticed, Cd(II) ions present an initial rapid adsorption rate particularly with Cd-RTCS where the equilibrium was achieved after approximately 40 min, revealing the high affinity between the Cd(II) ions and the active coordination sites that were created within the Cd-RTCS sorbent. Also, the higher adsorption of the Cd-RTCS compared to the NI-RTCS could be related to the integration of the coordination sites, which can selectively recognize and bind with Cd(II) ions.

Both the pseudo first-order and pseudo second-order equations were utilized in the mathematical analysis of the obtained kinetic data and they were expressed as in the following [44]:

Pseudo first order kinetic model

$$\ln (q_e - q_t) = \ln q_{el} - k_1 t \quad (7)$$

Pseudo second order kinetic model

$$\frac{1}{q_e} = \frac{1}{k_2 q_{e2}^2} + \frac{1}{q_e} \quad (8)$$

where q_e (mg/g) is the adsorbed Cd(II) ions quantity at equilibrium adsorption capacity in equilibrium; q_t (mg/g) is the adsorbed Cd(II) ions quantity at time t (min); k_1 (min^{-1}) and k_2 (g/mg min) are the pseudo first and second rate constants, respectively.

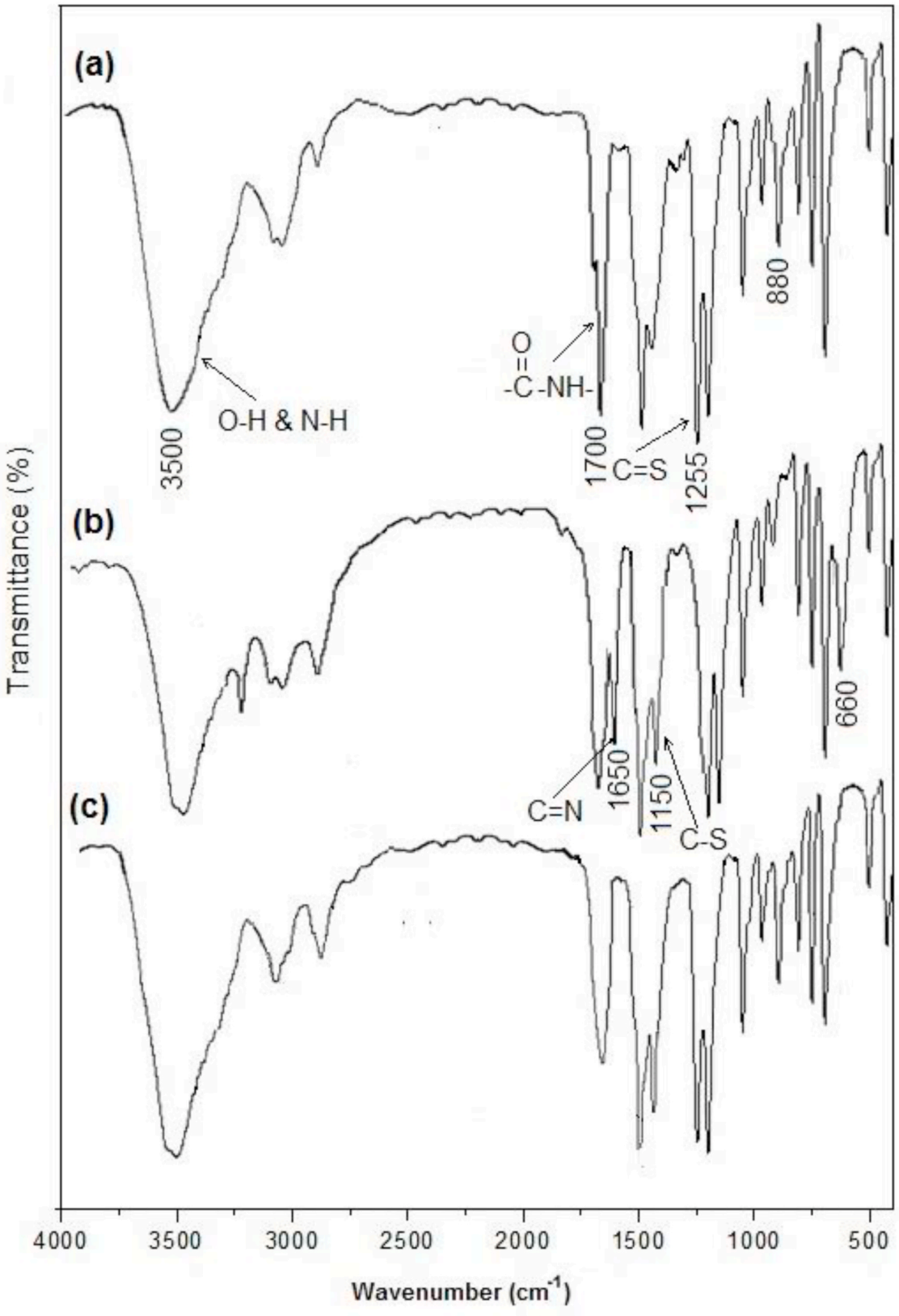

Fig. 5. FTIR spectra of (a) NI-RTCS (b) Cd(II) loaded Cd-RTCS, and (c) Cd(II) free Cu-PIS

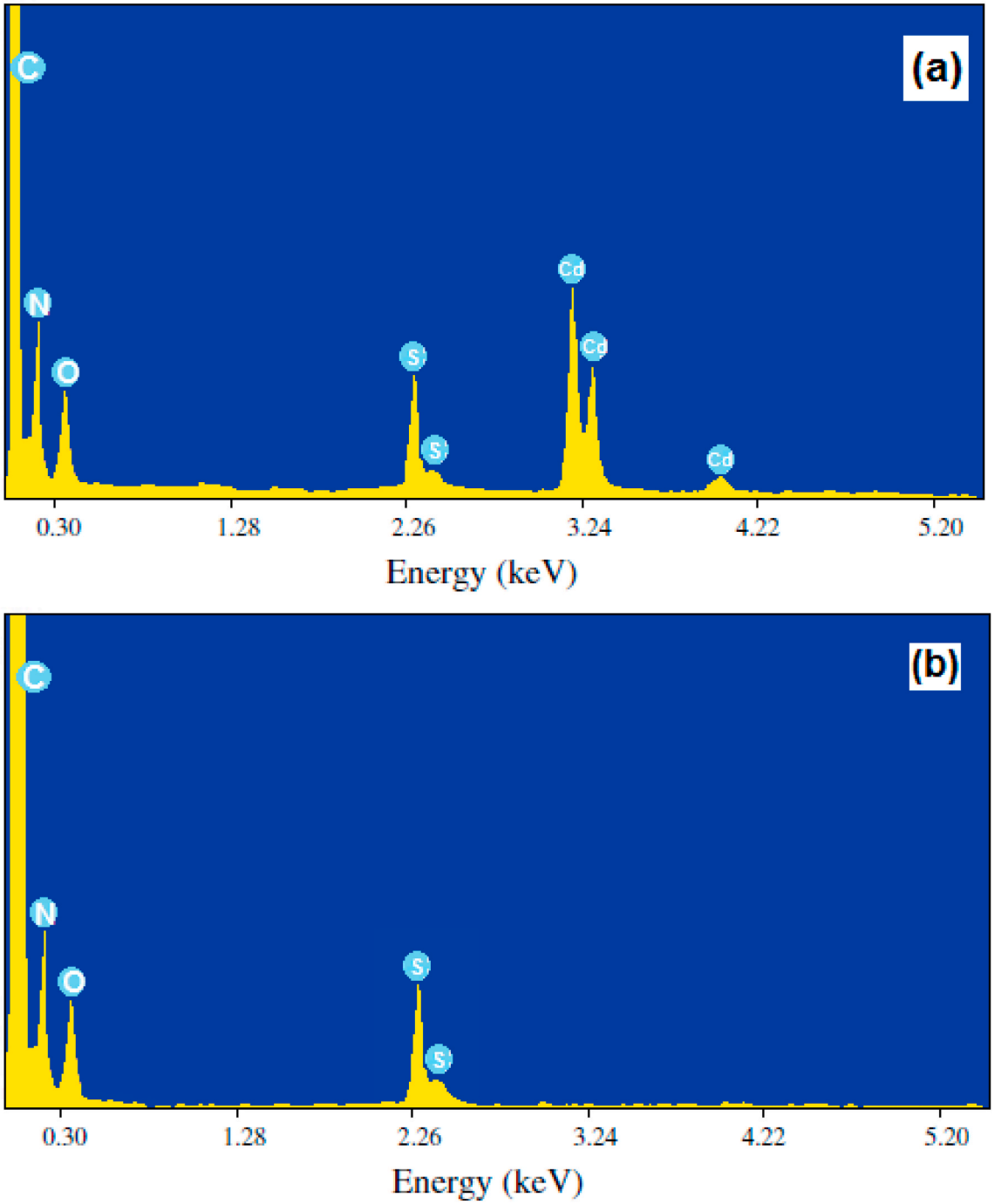

Fig. 6. EDX spectra of imprinted Cd-RTCS (a) before and (b) after Cd(II) elution.

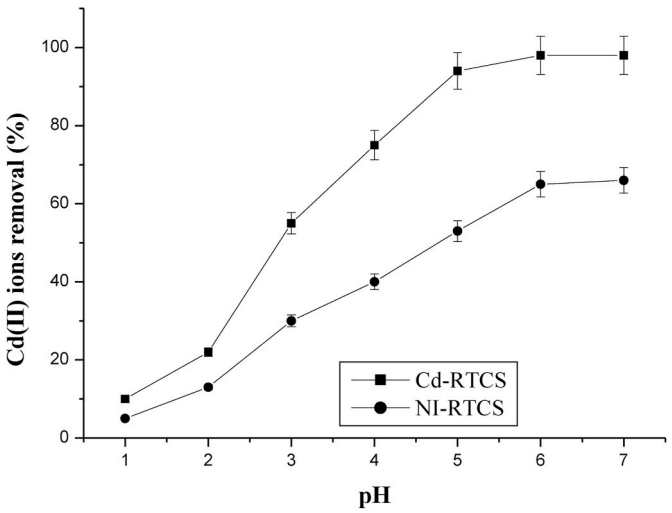

Fig. 7. Effect of pH on the Cd^{2+} ions removal by Cd-RTCS and NI-RTCS (initial concentration 200 mg/L; adsorbent. 1 g/L; contact time 3 h; shaking rate 200 rpm, 30 °C).

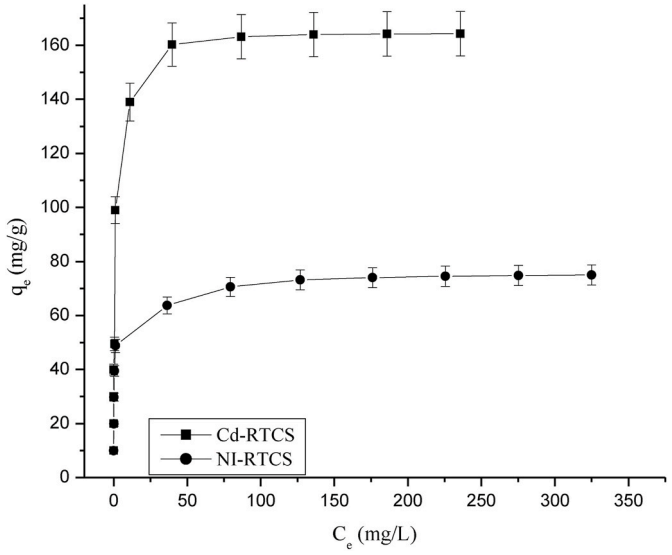

Fig. 8. Effect of initial concentration on the uptake of Cd(II) ions by Cd-RTCS and NI-RTCS (adsorbent. 1 g/L; pH 6; contact time 3h shaking rate 200 rpm, 30 °C).

Table 5 presents all the kinetic constants of the Cd(II) ions uptake by Cd-RTCS and NI-RTCS sorbents that were obtained by applying the above equations along with the corresponding correlation coefficients (R^2) values. It is obvious that between the two models the highest R^2 values were observed with the pseudo-second-order equation, which indicates that the Cd(II) ions uptake process mainly relies on the accessibility to the coordination sites that were integrated with the sorbent surface and the chemical interaction via chelation of the Cd(II) ions by the thiosemicarbazide units is the rate-limiting step.

3.2.4. Selectivity study

The specific recognition capability of the Cd-RTCS for selective binding with Cd(II) was tested in presence of some common competitive ions including Pb(II), Ni(II), Zn(II), and, Cu(II), which were chosen on the bases of similar valence and close ionic size with our targeted Cd(II) ions. In such a highly interfering medium the main parameters that were calculated using Eqs. (2)–(4) including distribution coefficient (*D*), the selectivity coefficient ($\rho^{2+n+}_{Cd/M}$), and the relative selectivity coefficient (β_r) are presented in Table 6.

In the case of the Cd-RTCS adsorbent, both the distribution coefficient and selectivity coefficient values are significantly higher for Cd(II) ions than the other interfering ions, indicating a fact that the sorbent Cd-RTCS resin is able to selectively capture the Cd(II) ions when existing in such competitive medium containing these similar metal ions. On the other hand, the NI-RTCS sorbent resin didn't show any preference for binding to any of the existing ions more than others and for all metal ions, the relative selectivity coefficient values were >1. The aforementioned results can give clear evidence for the essential role of the utilized ion-imprinting technology in creating a noticeable selectivity in the constructed network of the Cd-RTCS resin.

3.2.5. Real Ni-Cd battery wastes sample treatment

After treating the solid waste of the Ni-Cd battery as previously shown in the experimental part, the initial Cd(II) and Ni(II) ions

Table 3
Maximum adsorption capacities for Cd(II) ions the adsorption by different adsorbents.

Adsorbent	q_m (mg/g)	Reference
Acrylamide functionalized ion-imprinted β-cyclodextrin	107	[9]
Modified ion-imprinted silica	41.2	[11]
Diatom-based Cd (II) ion-imprinted composite	5.5	[13]
4-vinyl pyridine modified ion-imprinted hybrid material	4.8	[31]
bis[3-(triethoxysilyl)propyl]tetrasulfide modified silica	22.2	[32]
Acrylamide functionalized ion-imprinted chitosan	167	[34]
Cd-RTCS (current work)	164	–

Table 4
Parameters for Cd(II) ions adsorption by Cd-RTCS and NI-RTCS resins according to different equilibrium models.

Resin	Langmuir isotherm constants		
	K_L(L/g)	q_m(mg/g)	R^2
Cd-RTCS	1.1×10^{-2}	164 ± 1	0.9997
NI- RTCS	8.5×10^{-3}	73 ± 1	0.9999
Resin	Freundlich isotherm constants		
	K_F	n	R^2
Cd-RTCS	55.21	.34	0.8988
NI- RTCS	43.35	3.18	0.8887

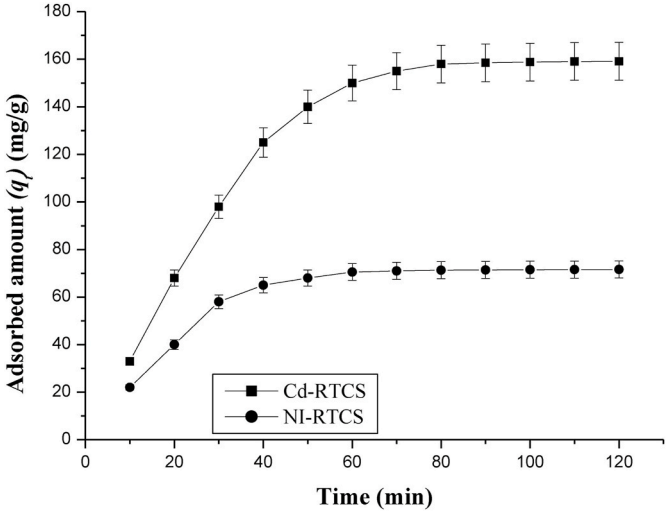

Fig. 9. Kinetic curve of the Cd(II) ions removal by Cd-RTCS, and NI-RTCS resins (initial concentration 200 mg/L, adsorbent 1 g/L, pH 6.0, shaking rate 200 rpm, 30 °C).

Table 5
Kinetic parameters for Cd(II) ions extraction by Cd-RTCS and NI-RTCS adsorbents.

Adsorbent	First-order model		
	k_1 (min^{-1})	q_{e1}(mg/g)	R^2
Cd-RTCS	0.113	158 ± 2	0.8773
NI-RTCS	0.153	68 ± 3	0.8782
Adsorbent		Second-order model	
	k_2 (g/(mg min))	q_{e2} (mg/g)	R^2
Cd-RTCS	2.4×10^{-4}	161 ± 0.5	0.9988
NI-RTCS	2.7×10^{-4}	70 ± 1	0.9889

Table 6
Selective adsorption of Cd(II) from multi-component mixtures by Cd-RTCS and NI- RTCS resins (initial concentration 30 mg/L, adsorbent 1 g/L, shaking rate 200 rpm, solution pH 6.0, 30 °C).

Metal	Distribution ratio (L/g)		Selectivity coefficient $\beta^{2+n+}_{Cd/M}$		Relative selectivity coefficient β_r
	Cd-RTCS	NI-RTCS	Cd-RTCS	NI-RTCS	
Cd^{2+}	612.4	22.7	–	–	
Pb^{2+}	26.6	21.5	23.02	1.06	21.72
Ni^{2+}	30.4	23.7	20.15	0.96	20.99
Zn^{2+}	20.3	15.1	30.17	1.50	20.11
Cu^{2+}	34.5	25.6	17.75	0.88	20.17

concentrations were respectively estimated at 85 and 68 mg/L. Fig. 10 presents the percent removal of both Cd(II) and Ni(II) ions after shaking the waste solution individually with either Cd-RTCS or NI-RTCS sorbents in two separate batches and as can be seen, in the case of NI-RTCS, the percent removal values of both Cd(II) and Ni(II) ions were approximately 33% and 35% revealing almost similar tendencies of the non-imprinted sorbent resin toward the two metals. On the other hand, the Cd-RTCS sorbent batch demonstrated percent removal values around 97% and 9% for both Cd(II) and Ni(II) ions, which confirm the high efficiency of the employed Cd(II) ion-imprinting technique in creating considerable selective capabilities within the construction of the prepared Cd-RTCS resin toward the targeted Cd(II) ions.

3.2.6. Reusability

Assessment of adsorbent regeneration and reusability is essential to estimate utility life and functional damage that can occur after each reuse cycle. In the current study, the Cd-RTCS resin sample was employed in 5 Cd(II) ions removal cycles (Fig. 11) and upon each time the resin was regenerated by 0.1 M HNO_3. Cd(II) capacity was determined each time and did not show a significant decrease over the five cycles. After the last cycle, the capacity of the Cd-RTCS resin was about 96% of that of the initial capacity obtained in the first cycle.

4. Conclusions

A durable phenolic resin was developed on the basis of ion-imprinting strategy and demonstrated a high potential for selective uptake of Cd(II) ions among other interfering metal ions. The phenolic ligand H_2TCS was first prepared by thiosemicarbazide modification of salicyloyl hydrazide, which can effectively coordinate with the Cd(II) and form a stable [CdTCS(H_2O)$_3$] complex that was polymerized with resorcinol and formalin. The formed resinous material was eluted by 0.1 M HNO_3 to remove the incorporated Cd(II) ions to finally obtain the selective Cd-RTCS sorbent resin. The simple H_2TCS and the complex [CdTCS(H_2O)$_3$] was characterized by instrumental techniques to confirm their chemical structures. Also, the resin materials were examined using SEM and FTIR spectroscopy. The maximum capacity of the Cd-RTCS that was anticipated from the isotherm experiment was 164 ± 1 mg/g and the adsorption was interpreted by the Langmuir model. Moreover, the capability of the Cd-RTCS resin for selective capturing of Cd(II) was tested in presence of some common competitive ions including Pb(II), Ni(II), Zn(II), and, Cu(II) and all the calculated parameters indicated the usefulness of the ion-imprinted technique in generating a considerable Cd(II) ions selectivity.

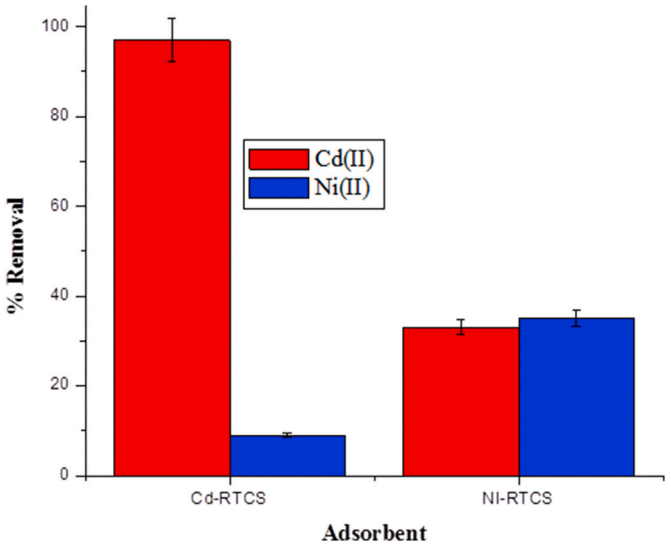

Fig. 10. % Removal of Cd(II) and Ni(II) ions from the real waste sample from Ni-Cd battery using Cd-RTCS and NI-RTCS.

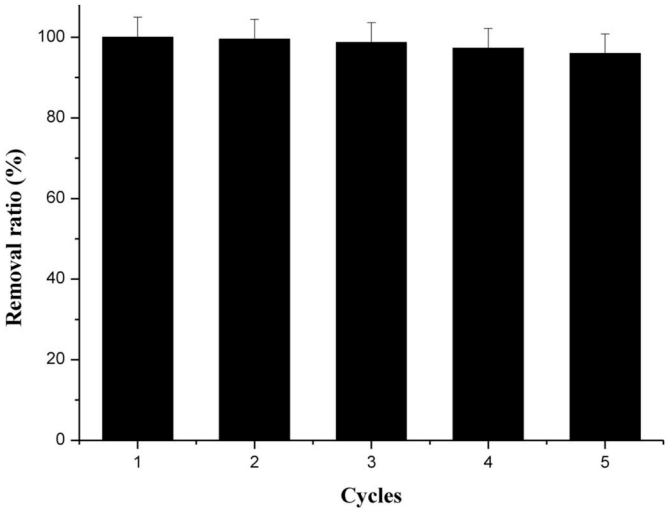

Fig. 11. Reusability of Cd-RTCS resin.

CRediT authorship contribution statement

Nadia H. Elsayed: designed the research study. performed the research. analyzed the data. All the authors declare that there is no any conflict of interest. **M. Monier:** designed the research study. contributed essential reagents and tools. analyzed the data. wrote the paper. All the authors declare that there is no any conflict of interest. **Raedah A.S. Alatawi:** performed the research. contributed essential reagents and tools. wrote the paper. All the authors declare that there is no any conflict of interest.

Declaration of competing interest

The authors declare that they have no known competing financial

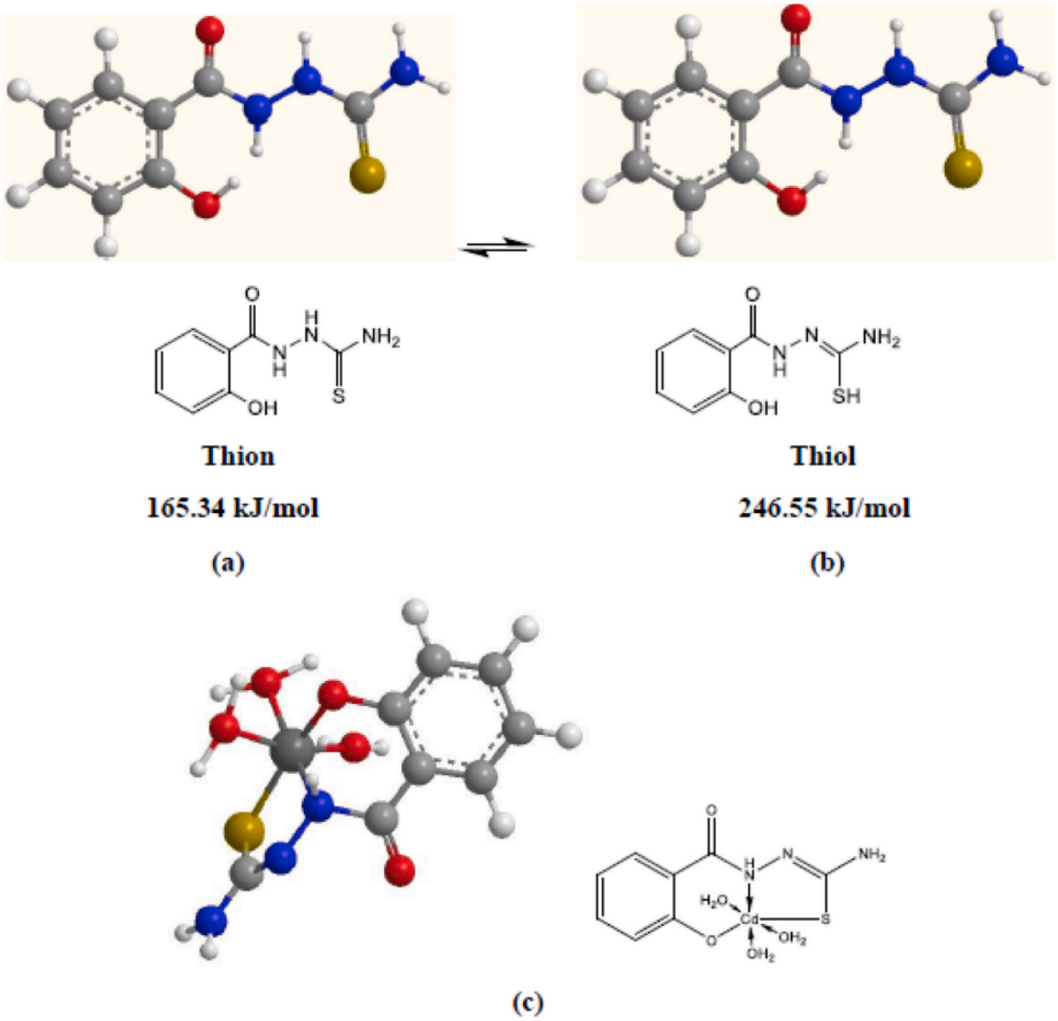

Structure 1. Molecular model of (a) thion, (b) thiol forms, and (c) [CdTCS$(H_2O)_3$].

interests or personal relationships that could have appeared to influence the work reported in this paper.

Acknowledgment

The authors extend their appreciation to the deanship of Scientific Research at University of Tabuk for funding this work through research group number RGP S-1441-0021.

References

[1] K. Huang, Y. Chen, F. Zhou, X. Zhao, J. Liu, S. Mei, Y. Zhou, T. Jing, Integrated ion imprinted polymers-paper composites for selective and sensitive detection of Cd(II) ions, J. Hazard Mater. 333 (2017) 137–143.
[2] H. Chen, X. Yang, P. Wang, Z.X. Wang, M. Li, F.J. Zhao, Dietary cadmium intake from rice and vegetables and potential health risk: a case study in Xiangtan, southern China, Sci. Total Environ. 639 (2018) 271–277.
[3] M. Ghanei-Motlagh, M.A. Taher, Novel imprinted polymeric nanoparticles prepared by sol–gel technique for electrochemical detection of toxic cadmium(II) ions, Chem. Eng. J. 327 (2017) 135–141.
[4] M. Hemmati, M. Rajabi, A. Asghari, Magnetic nanoparticle based solid-phase extraction of heavy metal ions: a review on recent advances, Mikrochim. Acta 185 (2018) 160–191.
[5] H. Yu, Z. Wang, R. Wu, X. Chen, T.D. Chan, Water-dispersible pH/thermo dual responsive microporous polymeric microspheres as adsorbent for dispersive solid phase extraction of fluoroquinolones from environmental water samples and food samples, J. Chromatogr. A 1601 (2019) 27–34.
[6] P. Kumar, A. Pournara, K.-H. Kim, V. Bansal, S. Rapti, M.J. Manos, Metal-organic frameworks: challenges and opportunities for ion-exchange/sorption applications, Prog. Mater. Sci. 86 (2017) 25–74.
[7] H. Jiang, N. Li, L. Cui, X. Wang, R. Zhao, Recent application of magnetic solid phase extraction for food safety analysis, TrAC Trends Anal. Chem. (Reference Ed.) 120 (2019) 115632–115646.
[8] H. Abdolmohammad-Zadeh, A. Salimi, Preconcentration of Pb(II) by using Mg(II)-doped $NiFe_2O_4$ nanoparticles as a magnetic solid phase extraction agent, Mikrochim. Acta 185 (2018) 343–350.
[9] F. Zhu, L. Li, J. Xing, Selective adsorption behavior of Cd(II) ion imprinted polymers synthesized by microwave-assisted inverse emulsion polymerization: adsorption performance and mechanism, J. Hazard Mater. 321 (2017) 103–110.
[10] F. Shakerian, K.-H. Kim, E. Kwon, J.E. Szulejko, P. Kumar, S. Dadfarnia, A.M. Haji Shabani, Advanced polymeric materials: synthesis and analytical application of ion imprinted polymers as selective sorbents for solid phase extraction of metal ions, TrAC Trends Anal. Chem. (Reference Ed.) 83 (2016) 55–69.
[11] P. Yang, H. Cao, D. Mai, T. Ye, X. Wu, M. Yuan, J. Yu, F. Xu, A novel morphological ion imprinted polymers for selective solid phase extraction of Cd(II): preparation, adsorption properties and binding mechanism to Cd(II), React. Funct. Polym. 151 (2020), 104569.
[12] M. Monier, D.A. Abdel-Latif, D.A. Fabrication of Au(III) ion-imprinted polymer based on thiol-modifiedchitosan, Int. J. Biol. Macromol. 105 (2017) 777–787.
[13] Y. Miao, H. Zhang, Q. Xie, N. Chena, L. Ma, Construction and selective removal of Cd ion based on diatom-based Cd (II) ion-imprinted composite adsorbent, Colloids Surf. A Physicochem. Eng. Asp. 598 (2020), 124856.
[14] R. Keçili, E. Yılmaz, A. Ersöz, R. Say, Imprinted materials: from green chemistry to sustainable engineering, Sustain. Nanoscale Eng. (2020) 317–350.
[15] P.E. Hande, A.B. Samui, P.S. Kulkarni, Highly selective monitoring of metals by using ion-imprinted polymers, Environ. Sci. Pollut. Res. 22 (2015) 7375–7404.
[16] B. Sellergren (Ed.), Molecularly Imprinted Polymers: Man-Made Mimics of Antibodies and Their Application in Analytical Chemistry: Techniques and Instrumentation in Analytical Chemistry, Elsevier Science, Amsterdam, 2001.
[17] J. Kupai, M. Razali, S. Büyüktiryaki, R. Keçili, G. Szekely, Long-term stability and reusability of molecularly imprinted polymers, Polym. Chem. 8 (2017) 666–673.
[18] R. Keçili, C.M. Hussain, Recent progresses of imprinted nanomaterials in analytical chemistry, Int. J. Anal. Chem. (2018), 8503853.

[19] X. Xu, M. Wang, Q. Wu, Z. Xu, X. Tian, Synthesis and application of novel magnetic ion-imprinted polymers for selective solid phase extraction of cadmium (II), Polymja 9 (8) (2017) 360–368.
[20] R. Keçili, İ. Dolak, B. Ziyadanoğulları, A. Ersöz, R. Say, Ion imprinted cryogel-based supermacroporous traps for selective separation of cerium(III) in real samples, J. Rare Earths 36 (8) (2018) 857–862.
[21] İ. Dolak, R. Keçili, D. Hür, A. Ersöz, R. Say, Ion imprinted polymers for selective recognition of neodymium (III) in environmental samples, Ind. Eng. Chem. Res. 4 (2015) 5328–5335.
[22] C. Branger, W. Meouche, A. Margaillan, Recent advances on ion-imprinted polymers, React. Funct. Polym. 73 (2013) 859–875.
[23] L.D. Marestoni, M.D.P.T. Sotomayor, M.G. Segatelli, L.R. Sartori, C.R.T. Tarley, Polímeros impressos com íons: fundamentos, estratégias de preparo e aplicações em química analítica, Quim. Nova 36 (2013) 1194–1207.
[24] F. Shakerian, K.-H. Kim, E. Kwon, J.E. Szulejko, P. Kumar, S. Dadfarnia, A.M. Haji Shabani, Advanced polymeric materials: synthesis and analytical application of ion imprinted polymers as selective sorbents for solid phase extraction of metal ions, Trends Anal. Chem. 83 (2016), 55–TrAC 69.
[25] M.R. Alotaibi, M. Monier, N.H. Elsayed, Fabrication and investigation of gold (III) ion-imprinted functionalized silica particles, J. Mol. Recogn. 33 (2020), e2813.
[26] M. Monier, A.L. Shafik, D.A. Abdel-Latif, Synthesis of azo-functionalized ion-imprinted polymeric resin for selective extraction of nickel (II) ions, Polym. Int. 67 (2018) 1035–1045.
[27] M. Monier, D.A. Abdel-Latif, Synthesis of ion-imprinted microspheres based on carboxymethyl cellulose for selective removal of UO2 (II), Carbohydr. Polym. 97 (2013) 743–752.
[28] X. Cai, J. Li, Z. Zhang, F. Yang, R. Dong, L. Chen, Novel Pb^{2+} ion imprinted polymers based on ionic interaction via synergy of dual functional monomers for selective solid-phase extraction of Pb^{2+} in water samples, ACS Appl. Mater. Interfaces 6 (1) (2013) 305–313.
[29] J. He, H. Shang, X. Zhang, X. Sun, Synthesis and application of ion imprinting polymer coated magnetic multi-walled carbon nanotubes for selective adsorption of nickel ion, Surf. Sci. 428 (2018) 110–117.
[30] C.R.T. Tarley, F.N. Andrade, F.M. de Oliveira, M.Z. Corazza, L.F.M. de Azevedo, M. G. Segatelli, Synthesis and application of imprinted polyvinylimidazole-silica hybrid copolymer for Pb^{2+} determination by flow-injection thermospray flame furnace atomic absorption spectrometry, Anal. Chim. Acta 703 (2011) 145–151.
[31] C.R.T. Tarley, M.Z. Corazza, F.M. de Oliveira, B.F. Somera, C.C. Nascentes, M. G. Segatelli, On-line micro-solid phase preconcentration of Cd^{2+} coupled to TS-FFAAS using a novel ion-selective bifunctional hybrid imprinted adsorbent, Microchem. J. 131 (2017) 57–69.
[32] H.T. Fan, J.B. Wu, X.L. Fan, D.S. Zhang, Z.J. Su, F. Yan, T. Sun, Removal of cadmium (II) and lead (II) from aqueous solution using sulfur-functionalized silica prepared by hydrothermal-assisted grafting method, Chem. Eng. J. 198–199 (2012) 355–363.
[33] J. Wackerlig, R. Schirhagl, Applications of molecularly imprinted polymernanoparticles and their advances toward industrial use: a review, Anal. Chem. 88 (2016) 250–261.
[34] D. Rahangdale, A. Kumar, Acrylamide grafted chitosan based ion imprinted polymer for the recovery of cadmium from nickel-cadmium battery waste, J. Environ. Chem. Eng. 6 (2018) 1828–1839.
[35] O.A. Nurkenov, S.D. Fazylov, Zh B. Satpaeva, T.M. Seilkhanov, G. Zh Karipova, A. Zh Isaeva, Synthesis and structure of new derivatives of salicylic acid hydrazide, Russ. J. Gen. Chem. 84 (2014) 1574–1576.
[36] A.I. Vogel, Quantitative Inorganic Analysis, seventh ed., Longman, London, 2010.
[37] E.R.J. Nightingale, Phenomenological theory of ion solvation. Effective radii of hydrated ions, J. Phys. Chem. 63 (1958) 1381–1387.
[38] S. Emik, Preparation and characterization of an IPN type chelating resin containing amino and carboxyl groups for removal of Cu(II) from aqueous solutions, React. Funct. Polym. 75 (2014) 63–74.
[39] T.A. Yousef, G.M. Abu El-Reash, O.A. El-Gammal, R.A. Bedier, Synthesis, characterization, optical band gap, in vitro antimicrobial activity and DNA cleavage studies of some metal complexes of pyridyl thiosemicarbazone, J. Mol. Struct. 1035 (2013) 307–317.
[40] A.B.P. Lever, Inorganic Electronic Spectroscopy, Elsevier, Amsterdam, The Netherlands, 1968.
[41] H.M.F. Freundlich, Over the adsorption in solution, Z. Phys. Chem. 57 (1906) 385–471.
[42] I. Langmuir, The adsorption of gases on plane surfaces of glass mica and platinum, J. Am. Chem. Soc. 40 (1918) 1361–1403.
[43] M. Thommes, K. Kaneko, A.V. Neimark, J.P. Olivier, F. Rodriguez-Reinoso, J. Rouquerol, K.S.W. Sing, Physisorption of gases, with special reference to the evaluation of surface area and pore size distribution (IUPAC Technical Report), Pure Appl. Chem. 87 (2015) 1051–1069.
[44] Y.S. Ho, G. McKay, Pseudo-second-order model for sorption processes, Process Biochem. 34 (1999) 451–465.